

NASA/TM—2008-215462



Fatigue Behavior of a Third Generation PM Disk Superalloy

*John Gayda and Timothy P. Gabb
Glenn Research Center, Cleveland, Ohio*

October 2008

NASA STI Program . . . in Profile

Since its founding, NASA has been dedicated to the advancement of aeronautics and space science. The NASA Scientific and Technical Information (STI) program plays a key part in helping NASA maintain this important role.

The NASA STI Program operates under the auspices of the Agency Chief Information Officer. It collects, organizes, provides for archiving, and disseminates NASA's STI. The NASA STI program provides access to the NASA Aeronautics and Space Database and its public interface, the NASA Technical Reports Server, thus providing one of the largest collections of aeronautical and space science STI in the world. Results are published in both non-NASA channels and by NASA in the NASA STI Report Series, which includes the following report types:

- **TECHNICAL PUBLICATION.** Reports of completed research or a major significant phase of research that present the results of NASA programs and include extensive data or theoretical analysis. Includes compilations of significant scientific and technical data and information deemed to be of continuing reference value. NASA counterpart of peer-reviewed formal professional papers but has less stringent limitations on manuscript length and extent of graphic presentations.
- **TECHNICAL MEMORANDUM.** Scientific and technical findings that are preliminary or of specialized interest, e.g., quick release reports, working papers, and bibliographies that contain minimal annotation. Does not contain extensive analysis.
- **CONTRACTOR REPORT.** Scientific and technical findings by NASA-sponsored contractors and grantees.
- **CONFERENCE PUBLICATION.** Collected

papers from scientific and technical conferences, symposia, seminars, or other meetings sponsored or cosponsored by NASA.

- **SPECIAL PUBLICATION.** Scientific, technical, or historical information from NASA programs, projects, and missions, often concerned with subjects having substantial public interest.
- **TECHNICAL TRANSLATION.** English-language translations of foreign scientific and technical material pertinent to NASA's mission.

Specialized services also include creating custom thesauri, building customized databases, organizing and publishing research results.

For more information about the NASA STI program, see the following:

- Access the NASA STI program home page at <http://www.sti.nasa.gov>
- E-mail your question via the Internet to help@sti.nasa.gov
- Fax your question to the NASA STI Help Desk at 301-621-0134
- Telephone the NASA STI Help Desk at 301-621-0390
- Write to:
NASA Center for AeroSpace Information (CASI)
7115 Standard Drive
Hanover, MD 21076-1320

NASA/TM—2008-215462



Fatigue Behavior of a Third Generation PM Disk Superalloy

*John Gayda and Timothy P. Gabb
Glenn Research Center, Cleveland, Ohio*

National Aeronautics and
Space Administration

Glenn Research Center
Cleveland, Ohio 44135

October 2008

This report is a formal draft or working paper, intended to solicit comments and ideas from a technical peer group.

This report contains preliminary findings, subject to revision as analysis proceeds.

Trade names and trademarks are used in this report for identification only. Their usage does not constitute an official endorsement, either expressed or implied, by the National Aeronautics and Space Administration.

Level of Review: This material has been technically reviewed by technical management.

Available from

NASA Center for Aerospace Information
7115 Standard Drive
Hanover, MD 21076-1320

National Technical Information Service
5285 Port Royal Road
Springfield, VA 22161

Available electronically at <http://gltrs.grc.nasa.gov>

Fatigue Behavior of a Third Generation PM Disk Superalloy

John Gayda and Timothy P. Gabb
National Aeronautics and Space Administration
Glenn Research Center
Cleveland, Ohio 44135

Introduction

New powder metallurgy (PM) disk superalloys, such as ME3 (ref. 1), LSHR (ref. 2), and Alloy 10 (ref. 3), have been developed in recent years which enable rim temperatures in turbine disk applications to approach 1300 °F. Before these alloys can be utilized at 1300 °F their fatigue behavior at this temperature must be understood. For this reason fatigue tests were run on smooth and notched test bars under a variety of conditions. The notch tests included dwells at peak load to simulate service conditions in the rim of a modern gas turbine disk. The resulting fatigue lives were then analyzed in an initial attempt to rationalize fatigue behavior encountered under the various conditions studied in this paper.

Material and Procedures

The material selected for this program was LSHR, a 3rd generation PM superalloy, strengthened by approximately 55 percent gamma prime phase. The composition of LSHR is presented in table I. LSHR powder was produced using argon gas atomization and was consolidated by hot isostatic pressing and extrusion to produce 3 in. diameter billet. Mults cut from the billet were isothermally forged to produce pancake forgings about 6 in. in diameter and 1.6 in. in height. Forgings were subsequently heat treated utilizing a subsolvus solution step, 2070 °F/1h, fan cooled, and given a two step age, 1570 °F/4 h and 1425 °F/8 h. The resulting grain size was about ASTM 12 and the gamma prime distribution consisted of primary gamma prime about 1 μm, secondary gamma prime about 0.3 μm, and tertiary gamma prime less than 0.05 μm, as illustrated in figure 1. This heat treatment was selected based on the results of a previous study (4) which showed it to have a good balance of properties for gas turbine disk applications.

Standard mechanical tests were run at 1300 °F to verify the tensile and creep properties of the alloy. Tensile tests were run on both smooth and notched test specimens, the latter with an elastic stress concentration factor (K_t) of 2. Creep data was gathered using both smooth and notched test bars, the latter at the same K_t of 2. Stress relaxation tests were also run employing tensile specimens which were loaded to 1 percent strain and held there for 100 h.

As previously stated various fatigue tests were run at 1300 °F on this alloy. Smooth bar cyclic fatigue tests were run using both strain control and load control at 0.33 Hz for the first 24 h and 10 Hz thereafter. A minimum/maximum strain ratio of 0 was used in the strain controlled tests. Minimum/maximum load ratio (R) of 0 and -1 was employed in the load controlled tests. Load controlled 10 Hz notch fatigue tests were run using the geometry depicted in figure 2. The notch fatigue specimen again had a K_t of 2. The notch fatigue tests were run with and without a 90 sec dwell at peak load with $R = 0.05$.

Results and Discussion

Tensile and creep test results at 1300 °F are presented in tables II and III respectively. The smooth bar tensile and creep properties are in agreement with previous data for this heat treatment (ref. 4). The notched tensile strength was about 290 ksi, approximately 50 percent higher than the smooth bar strength, which is significantly higher than expected. Even more surprising was the comparison of creep and notch rupture lives. The notched specimens showed a consistent trend of significantly greater lives than the rupture lives of uniform gage specimens at the same applied net section stress level. Note, at 115 ksi, the notch rupture life was 620 h compared to 146 h for the smooth creep bar. More work, both experimental and analytical, is planned to understand this result. Stress relaxation data is presented in Figure 3. Stresses

near the yield strength of the alloy can be seen to drop quickly at this temperature and this factor will be significant in subsequent analysis of the data.

Fatigue test results are presented in table IV. The fatigue tests were run at various levels, which yielded lives of interest for gas turbine disk applications. The maximum and minimum stress data presented in the table for the strain controlled fatigue tests represent values at mid-life. Notch fatigue lives are tabulated as a function of applied net section stress (load/area at the base of the notch). Unlike the tensile and creep behavior of this alloy, the presence of a notch degrades fatigue life, as can be seen by comparing the lives of SMOOTH-7, $N_f = 41,245$ run at 0 to 150 ksi, and NOTCH-9, $N_f = 5,440$ run at 7 to 130 ksi. The application of a dwell at peak load in the notch test is clearly seen to further degrade life.

As stated in the beginning of this paper, the authors' goal is to rationalize the fatigue behavior of this alloy for the various test conditions studied herein. To start with, the fatigue data for the specimens without a notch were analyzed using a stress based Smith-Watson-Topper (SWT) approach (ref. 5) which factors in both stress amplitude and mean stress effects. The exact formulation of the SWT stress is shown below:

$$\sigma_{\text{SWT}} = ((\sigma_{\text{max}} - \sigma_{\text{min}}) * \sigma_{\text{max}}/2)^{0.5} \quad (1)$$

Figure 4 shows the results in which fatigue life is plotted against σ_{SWT} for all specimens without a notch. In general, the SWT approach does a good job of collapsing the data set, however, the effect of *R*-ratio for load controlled tests is still evident to a small extent.

To aid comparison of smooth and notched fatigue tests, finite element stress analyses of the notch specimens were run using ALGOR Software (ALGOR, Inc) employing a 2-D axisymmetric model shown in figure 5. Note that the nodes along the *y* and *z* axes were constrained to limit displacement parallel to the axes. The appropriate loading conditions were applied at the top of the model (arrows) to simulate the net section stress employed in the actual tests. The first series of analyses were run assuming a bilinear elastic-plastic material model using the following parameters:

| | |
|-----------------|-----------------------|
| Young's Modulus | 27×10^6 psi |
| Poisson's Ratio | 0.3 |
| Yield Point | 160×10^3 psi |
| Plastic Modulus | 300×10^3 psi |

These parameters were based on tensile stress-strain data summarized in table II. Figures 6 and 7 show the von Mises stress and strain distribution at peak load for the test run at 115 ksi. The von Mises formulation includes the effect of all stress/strain components for the complex stress state associated with the notch geometry. As expected, plastic flow is produced at the notch tip. After unloading, the von Mises stress and strain distributions, figures 8 and 9, exhibit residual stress and strain levels which are consistent with plastic flow at the notch tip. The axial stress distributions at maximum and minimum load are presented in figure 10, and clearly show a very high tensile stress at maximum load and a compressive stress at minimum load, which is again consistent with plastic flow at the notch tip. Subsequent analysis show little change in the analytical stress and strain distributions with continued cycling at maximum and minimum loads. Similar analyses were run for the other notch fatigue tests and the stabilized von Mises stresses at maximum and minimum loads are presented in table V for the critical element at the notch tip.

To compare lives of the smooth and notch fatigue tests, σ_{SWT} was also calculated for the notch fatigue tests using the von Mises stresses in table V. σ_{min} was assigned a negative value to reflect the compressive nature of the stress field near the notch at minimum load. The results of these calculations are summarized in table V. The life data for the notched specimens are plotted alongside the smooth data in figure 11. Clearly this methodology does not collapse the two datasets. For a given life the σ_{SWT} is greater for the notch specimens especially for longer lives. Finer grid density did not have a significant impact on stress levels as seen in figure 12.

The stress at the notch tip can relax at 1300 °F, thereby reducing the σ_{SWT} . A first order estimate of the stress relaxation at the notch tip can be made by choosing the viscoplastic stress analysis capability in the Algor Software. The same materials constants utilized in the elastic-plastic analysis are employed in the viscoplastic analysis, however, creep is included thru the use of a power law expression, $\Delta\varepsilon/\Delta t = A\sigma^n$. As seen in table VI, the notch fatigue lives lasted many thousands of cycles, but were always less than 10 h in duration since a test frequency of 10 Hz was employed to minimize cost. To estimate peak stress at half life, the viscoplastic analysis was conducted using a fixed time increment of 0.01 h and a single cycle whose period was equated to the specimen life in column 5 of table VI. Values of $n = 5$ and $A = 1e-28h^{-1}$ in the power law expression for creep were employed to provide reasonable estimates of the upper portion of the relaxation curve in figure 3. The degree of stress relaxation was substantial, as can be seen in figure 13, where the von Mises stress distribution at the notch tip is compared for the elastic-plastic and the viscoplastic analyses under identical loads. Estimates of the maximum and minimum von Mises stresses as a function of applied loads, using the viscoplastic analysis, are summarized in table VI. From these values, the σ_{SWT} was calculated and plotted against life in figure 14. Note that the life lines for the smooth and notch data are significantly closer especially at the lower stress levels. Clearly, the life lines remain distinct, and other factors persist which preclude complete unification of the smooth and notch fatigue life datasets. These factors may include, but are not necessarily limited to, environmental effects associated with differences in test frequency, stress-volume effects, as well as the approximations used in calculating the multiaxial stress state at the notch tip.

To understand notch dwell fatigue behavior, an assessment of the notch tip stress distribution was again performed using the viscoplastic analysis. To provide estimates of stresses and strains at half life and failure, two dwell cycles were used to simulate these tests, with the dwell time for each cycle set equal to one half the total test time (life) shown in column 3 of table VII. As the time to failure is much greater than 10 h, the value of A in the power law creep expression was lowered to $3e-30h^{-1}$ to more accurately represent the lower portion of the relaxation curve in figure 3 and a time increment of 0.1 h was employed in the analyses. The resulting estimate of the von Mises stress distribution at the beginning and the end of the 115 ksi notch dwell fatigue test is presented in figure 15. Note the stresses at the onset of testing produce yielding at the notch tip but relax to levels near 100 ksi by the end of the test. This decrease in peak stress would tend to indicate dwell notch fatigue lives should equal or exceed that of the notch fatigue lives, which is clearly not the case. However, this relaxation of stresses at the notch tip is also accompanied by a corresponding increase in strain. As seen in figure 16, the von Mises strain at the notch tip reaches levels around 5 percent at the end of the test. This represents a significant fraction of the alloy's elongation at 1300 °F. The exact results of the peak von Mises stress at half life, used to estimate fatigue damage, and the peak von Mises strain at failure, used to estimate creep damage, is summarized in table VII, along with the initial values for these parameters for all notch dwell fatigue tests. These results suggest that creep damage should be more pronounced in tests at lower stresses while fatigue damage should be more pronounced in tests at higher stresses.

To assess the creep-fatigue damage hypothesis without undo reliance on the estimated notch tip stress and strain fields, the notch dwell fatigue data was analyzed using the applied net section stress and a simple linear creep-fatigue damage law shown below:

$$1 = n/N_f + t/T_f \quad (2)$$

| | |
|-------|---|
| n | number of notch dwell fatigue cycles |
| t | time ($t = \text{dwell time} \times n$) |
| N_f | experimental notch fatigue life |
| T_f | experimental notch rupture life |

The experimental data for the notch fatigue and notch rupture lives are plotted in figures 17 and 18 respectively as a function of applied net section stress. The best fit lines in these plots were used to obtain N_f and T_f in the creep-fatigue damage law. As both these tests were also run in air, environmental effects

are incorporated in the baseline fatigue and creep test data. If one inserts values for the notch dwell fatigue life, n , the notch fatigue life, N_f , and the notch rupture life, T_f , as a function of applied net section stress in the above equation, a measure of deviation from the creep-fatigue damage law can be obtained. The results of these calculations are summarized in table VIII. As seen in this table, the calculated deviation is close to unity, which represents perfect agreement between experiment and theory. Even the test at 130 ksi with a deviation between experiment and theory of 0.44 is good for fatigue data, where 2x scatter in life is often observed. Table VIII also includes the calculated creep life fraction, t/T_f , for each notch dwell fatigue test. At lower stresses, the creep life fraction constitutes a majority of the calculated deviation from equation (2), which indicates that a majority of the life is consumed by creep damage at lower stresses. At higher stresses, fatigue damage predominates. Overall this simplistic analysis of the notch dwell fatigue test data was quite successful given the complexity of these tests.

Summary and Conclusions

The fatigue behavior of a 3rd generation PM disk alloy, LSHR, was studied at 1300 °F. Tensile, creep, and fatigue tests were run on smooth and notched ($K_t = 2$) bars under a variety of conditions. Analysis of smooth bar fatigue data, run under strain and load control with R ratios of 0 and -1 , showed that a stress based Smith-Watson-Topper approach could collapse the data set. While the tensile and creep data showed substantial notch strengthening at 1300 °F, the fatigue data showed a life deficit for the notch specimens. A viscoplastic finite element model, which accounted for stress relaxation at the notch tip, provided the best correlation between the notched and smooth bar behavior, although the fatigue data was not fully rationalized based on this simplified viscoplastic model of the stresses at the notch tip.

Inclusion of a 90 sec dwell at peak load was found to dramatically decrease notch fatigue life. This result was shown to be consistent with a simple linear creep-fatigue damage rule, where creep damage dominated at low stresses and fatigue damage was more prevalent at higher stresses.

References

1. T. Gabb, J. Telesman, P. Kantzos, and K. O'Connor, "Characterization of the Temperature Capability of Advanced Disk Alloy ME3," NASA/TM—2002-211796, August 2002.
2. T. Gabb, J. Gayda, J. Telesman, and P. Kantzos, "Thermal and Mechanical Property Characterization of the Advanced Disk Alloy LSHR," NASA/TM—2005-213645, June 2005.
3. S. Jain, "Regional Engine Disk Process Development," NASA Contract NAS3-27720, September 1999.
4. J. Gayda, T. Gabb, and J. Telesman, "Notch Fatigue Strength of a PM Disk Superalloy," NASA/TM—2007-215046, October 2007.
5. K. Smith, P. Watson, and T. Topper, "A Stress-Strain Function for the Fatigue of Metal," Journal of Materials, pp. 767-778, December 1970.

TABLE I.—COMPOSITION OF NICKEL-BASE SUPERALLOY LSHR IN WEIGHT PERCENT

| Co | Cr | Al | Ti | Mo | W | Nb | Ta | C | B | Zr |
|------|------|-----|-----|-----|-----|-----|-----|------|------|------|
| 21.3 | 12.9 | 3.4 | 3.6 | 2.7 | 4.3 | 1.4 | 1.7 | 0.03 | 0.03 | 0.05 |

TABLE II.—1300 °F TENSILE RESULTS

| Tensile | Yield (ksi) | UTS (ksi) | Elongation (%) |
|---------------|-------------|-----------|----------------|
| E2-T1 | 161 | 189 | 9.5 |
| E2-T2 | 165 | 191 | 8.0 |
| Notch tensile | Kt | UTS (ksi) | |
| C-NT1 | 2 | 288 | *** |
| C-NT2 | 2 | 296 | *** |

TABLE III.—1300 °F CREEP RESULTS

| Creep | Stress (ksi) | 0.2% strain (h) | Rupture life (h) | Elongation (%) |
|---------------|--------------|-----------------|------------------|----------------|
| E2-C1 | 70 | 237 | 1532 | 9.7 |
| E2-C2 | 100 | 34 | 262 | 6.9 |
| E2-C3 | 115 | 12 | 146 | 9.5 |
| E2-C4 | 130 | 2 | 35 | 7.9 |
| Notch rupture | Stress (ksi) | Kt | Rupture life (h) | |
| E2-NR1 | 100 | 2 | 1105 | *** |
| E2-NR2 | 115 | 2 | 620 | *** |
| E2-NR3 | 130 | 2 | 313 | *** |

TABLE IV.—1300 °F FATIGUE RESULTS

| Spec | Control | Dwell | Strain (%) | Max σ (ksi) | Min σ (ksi) | Life (cycles) |
|-----------|---------|--------|------------|--------------------|--------------------|---------------|
| Smooth-1 | Strain | No | 1.00 | 146 | -95 | 1442 |
| Smooth-2 | Strain | No | 0.80 | 144 | -53 | 25959 |
| Smooth-3 | Strain | No | 0.60 | 133 | -19 | 69675 |
| Smooth-4 | Strain | No | 0.60 | 124 | -28 | 162903 |
| Smooth-5 | Load | No | *** | 180 | 0 | 1913 |
| Smooth-6 | Load | No | *** | 160 | 0 | 17418 |
| Smooth-7 | Load | No | *** | 150 | 0 | 41245 |
| Smooth-8 | Load | No | *** | 130 | -130 | 6296 |
| Smooth-9 | Load | No | *** | 120 | -120 | 20054 |
| Smooth-10 | Load | No | *** | 110 | -110 | 223010 |
| Notch-1 | Load | 90 sec | *** | 115 | 5.8 | 37361 |
| Notch-2 | Load | 90 sec | *** | 115 | 5.8 | 38280 |
| Notch-3 | Load | 90 sec | *** | 120 | 6 | 13443 |
| Notch-4 | Load | 90 sec | *** | 130 | 7 | 2123 |
| Notch-5 | Load | No | *** | 115 | 5.8 | 245105 |
| Notch-6 | Load | No | *** | 115 | 5.8 | 297795 |
| Notch-7 | Load | No | *** | 120 | 6 | 102317 |
| Notch-8 | Load | No | *** | 125 | 6 | 38300 |
| Notch-9 | Load | No | *** | 130 | 7 | 5440 |

TABLE V.—VON MISES STRESSES BASED ON ELASTIC-PLASTIC ANALYSIS OF NOTCH FATIGUE SPECIMENS

| Max σ (ksi) | Min σ (ksi) | Max von Mises σ | Min von Mises σ | SWT von Mises σ |
|-----------------------|-----------------------|---------------------------|---------------------------|---------------------------|
| 115 | 5 | 164 | 42 | 130 |
| 120 | 6 | 164 | 50 | 132 |
| 125 | 6 | 165 | 59 | 136 |
| 130 | 7 | 165 | 67 | 138 |

TABLE VI.—1300 °F NOTCH FATIGUE DATA AND VON MISES STRESSES BASED ON VISCOPLASTIC ANALYSIS

| Spec | Max σ (ksi) | Min σ (ksi) | Life (cycles) | Life (h) | Max von Mises σ | Min von Mises σ | SWT von Mises σ |
|---------|-----------------------|-----------------------|------------------|-------------|---------------------------|---------------------------|---------------------------|
| Notch-5 | 115 | 5 | 245105 | 6.8 | 131 | 76 | 116 |
| Notch-6 | 115 | 5 | 297795 | 8.3 | 128 | 77 | 115 |
| Notch-7 | 120 | 6 | 102317 | 2.8 | 138 | 79 | 122 |
| Notch-8 | 125 | 6 | 38300 | 1.1 | 151 | 77 | 131 |
| Notch-9 | 130 | 7 | 5440 | 0.2 | 162 | 72 | 138 |

TABLE VII.—VON MISES (VM) STRESSES AND STRAINS OF NOTCH DWELL FATIGUE SPECIMENS BASED ON VISCOPLASTIC ANALYSIS

| Spec | Dwell stress (ksi) | Life (h) | Initial VM σ | Initial VM ϵ | Half life VM σ | Full life VM ϵ |
|---------|-----------------------|-------------|------------------------|--------------------------|--------------------------|----------------------------|
| Notch-1 | 115 | 934 | 159 | 0.012 | 113 | 0.068 |
| Notch-2 | 115 | 957 | 159 | 0.012 | 113 | 0.068 |
| Notch-3 | 120 | 336 | 159 | 0.013 | 118 | 0.044 |
| Notch-4 | 130 | 53 | 164 | 0.015 | 138 | 0.026 |

TABLE VIII.—PREDICTION OF NOTCH DWELL FATIGUE LIFE

| Notch stress (ksi) | Rupture life, T_f (h) | Fatigue life, N_f (cycles) | Dwell fatigue life (cycles) | Deviation from predicted life (1=perfect) | Creep fraction t/T_f |
|-----------------------|----------------------------|---------------------------------|--------------------------------|---|---------------------------|
| 115 | 680 | 300000 | 37361 | 1.49 | 1.37 |
| 115 | 680 | 300000 | 38280 | 1.53 | 1.41 |
| 120 | 550 | 85000 | 13443 | 0.77 | 0.61 |
| 130 | 290 | 8000 | 2123 | 0.45 | 0.18 |

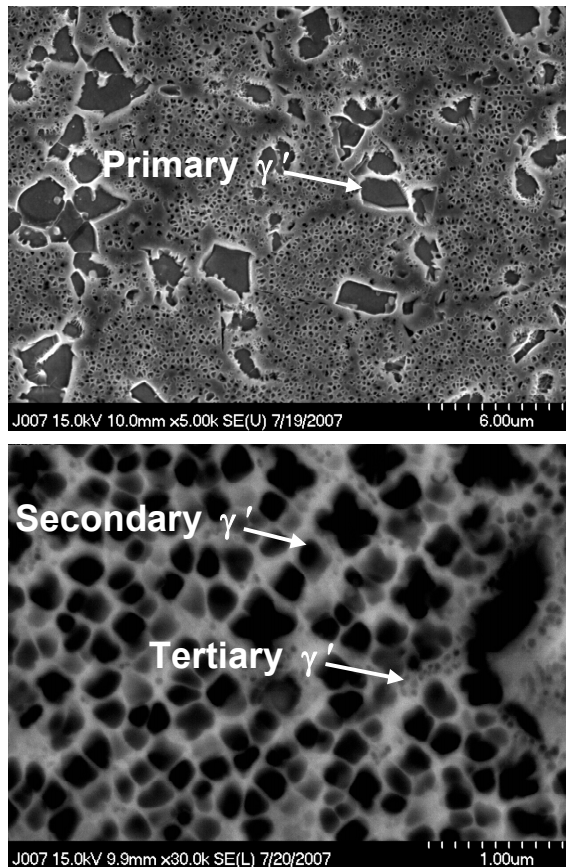


Figure 1.—Microstructure of the LSHR alloy.

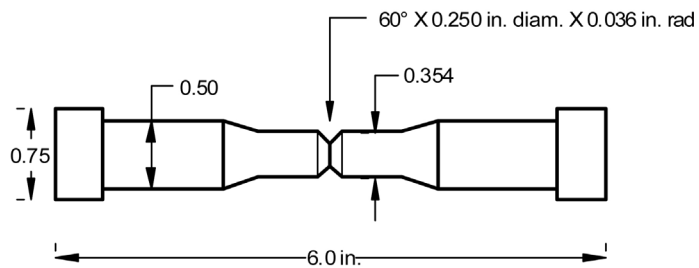


Figure 2.—Design of the notch fatigue specimen ($K_t = 2$). The notch was machined by low stress grinding, followed by polishing parallel to the specimen centerline.

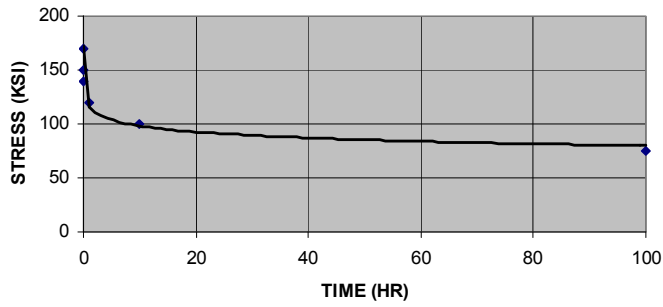


Figure 3.—Stress relaxation data.

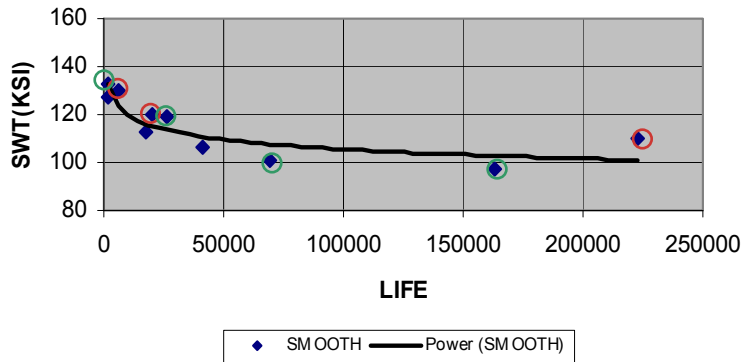


Figure 4.—1300 °F SWT fatigue life plot. Load controlled data with $R = -1$ shown circled in red. Strain controlled data shown circled in green.

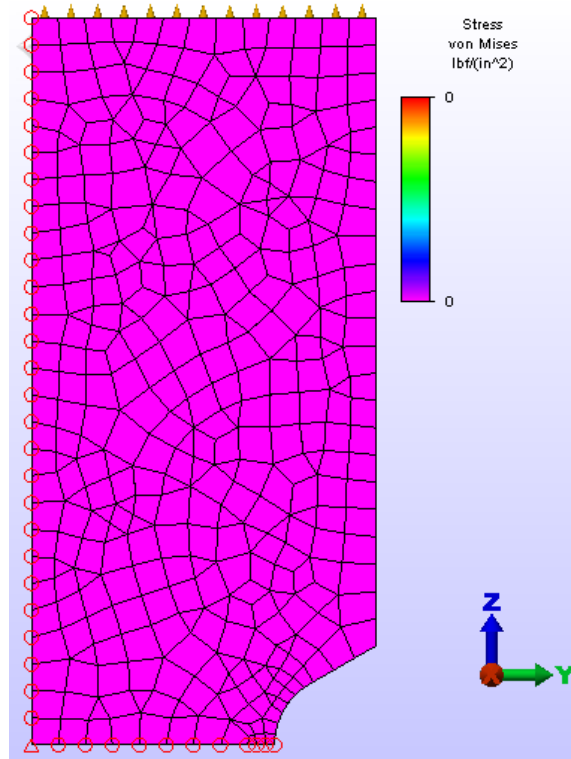


Figure 5.—Finite element mesh used in analyses of notch specimen.

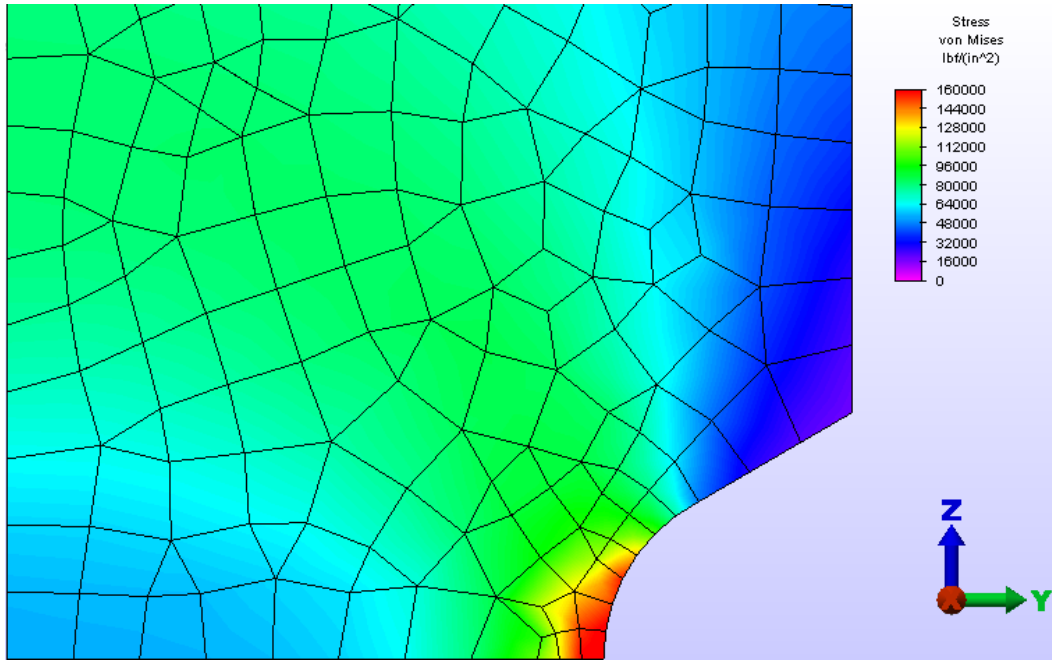


Figure 6.—Von Mises stresses at peak load.

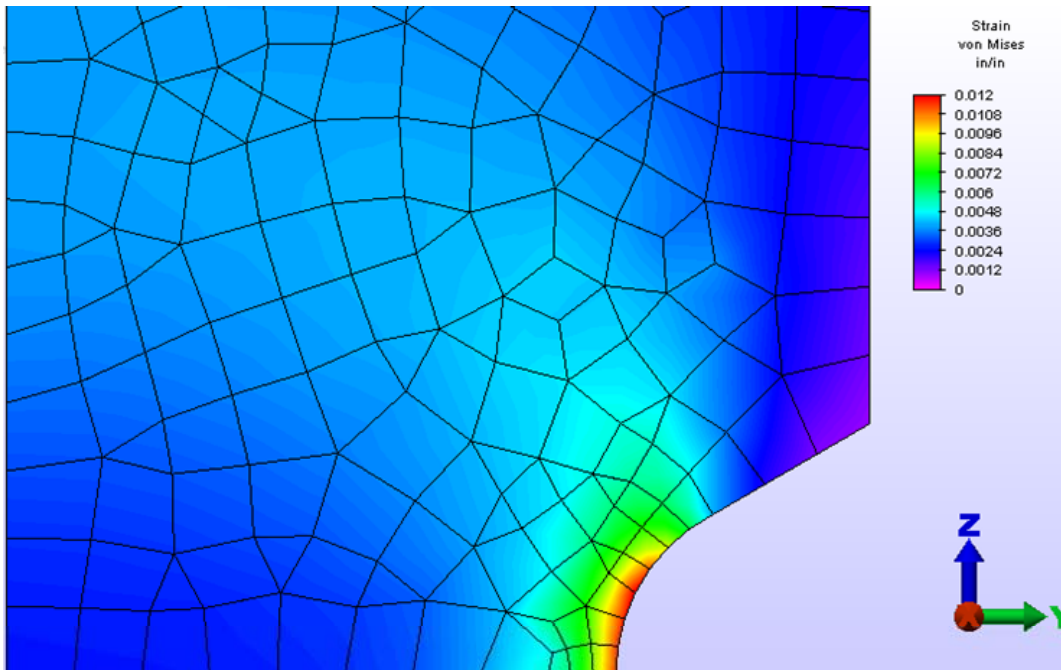


Figure 7.—Von Mises strains at peak load.

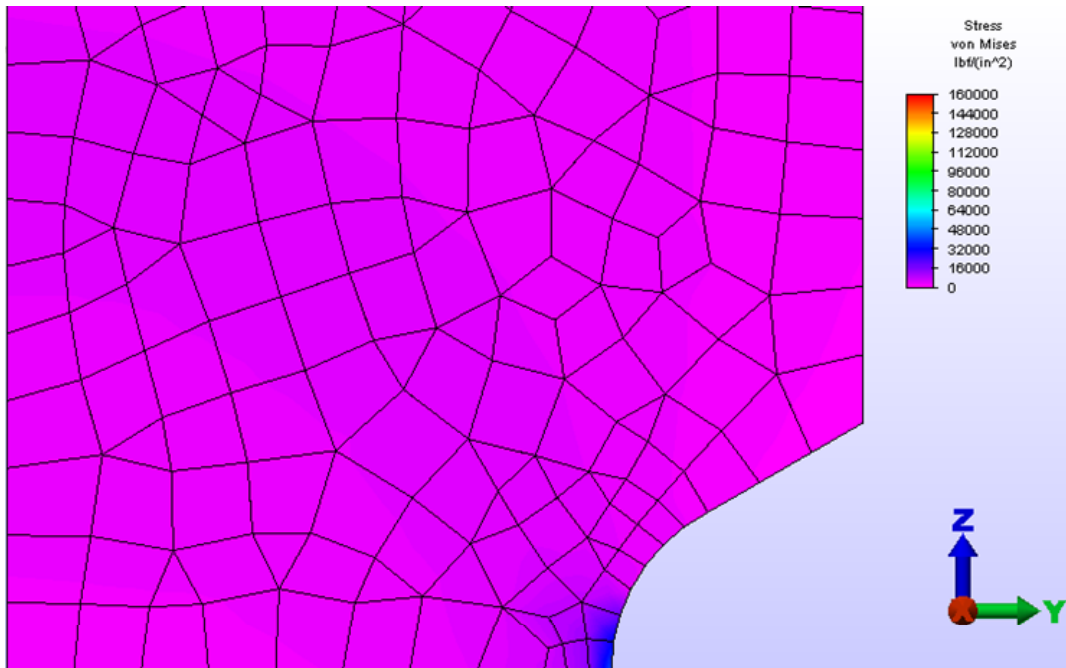


Figure 8.—Von Mises stresses after unloading.

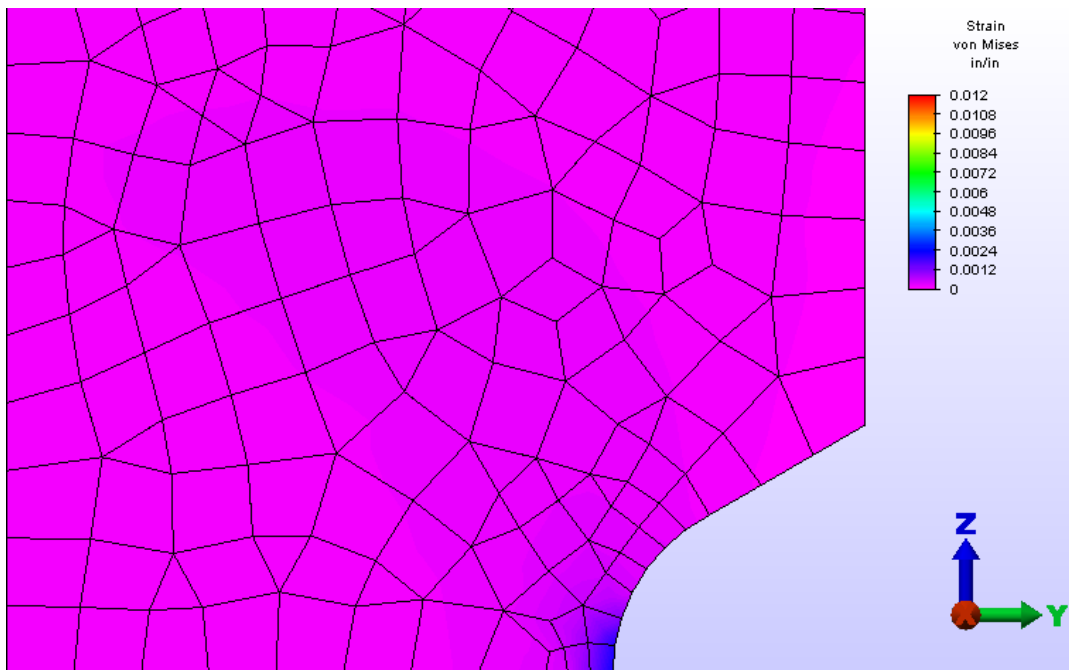


Figure 9.—Von Mises strains after unloading.

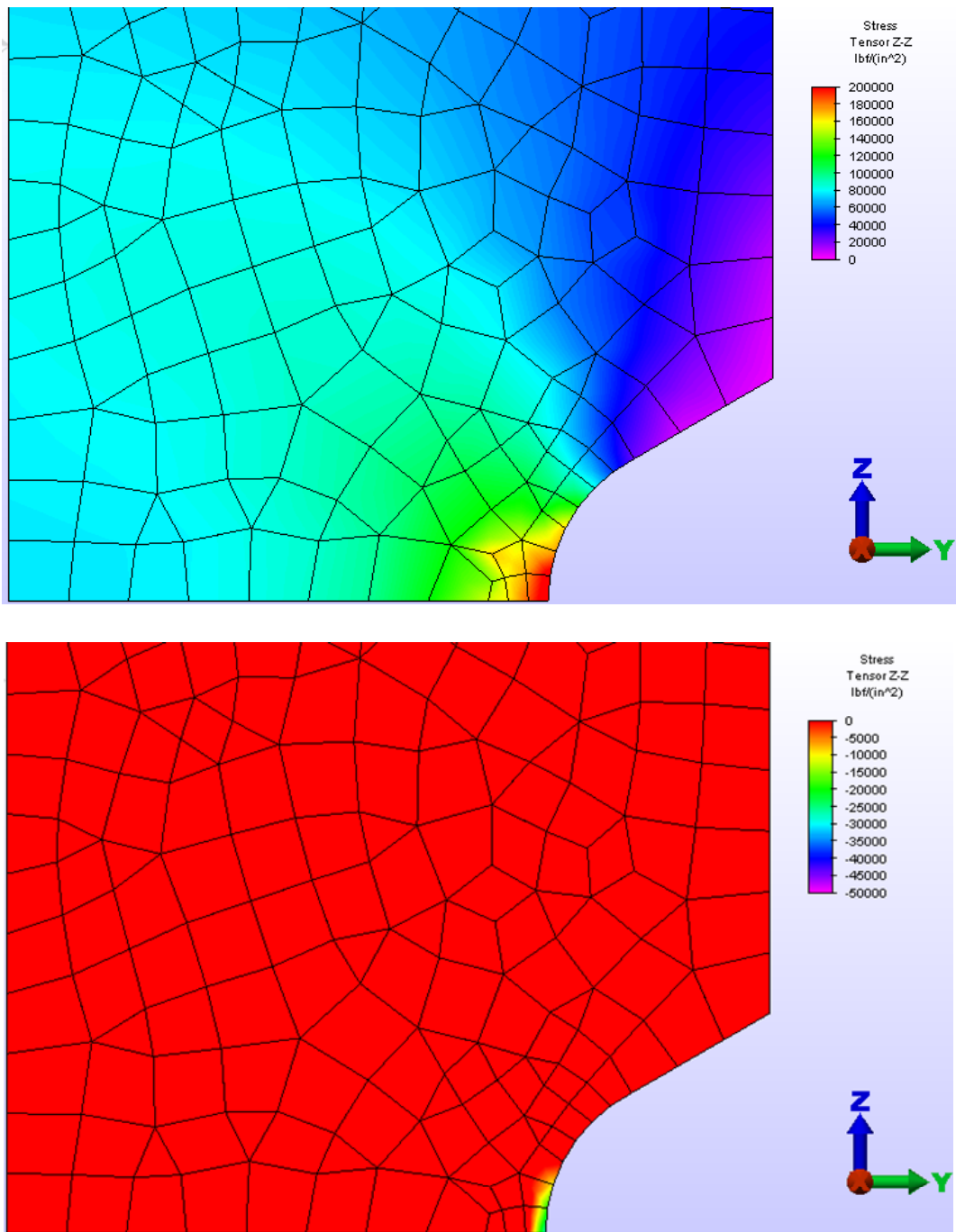


Figure 10.—Axial stresses at max (top) and min (bottom) load.

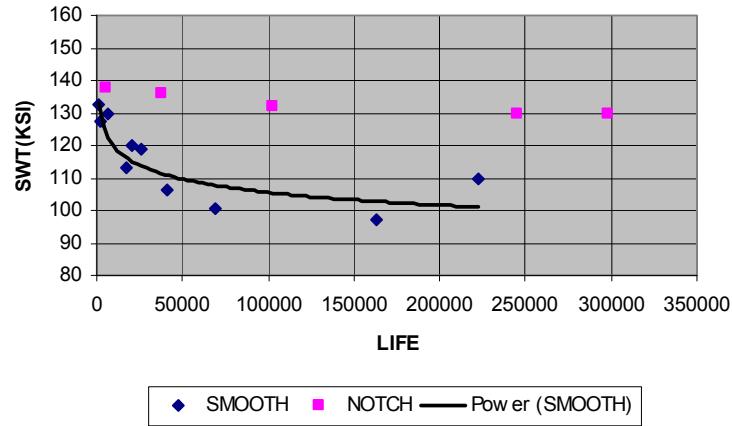


Figure 11.—1300 °F SWT fatigue life plot showing notch data based on elastic-plastic finite element stress analysis.

| Mesh density | Max von Mises (ksi) | Min von Mises (ksi) | Von Mises SWT (ksi) |
|--------------|---------------------|---------------------|---------------------|
| Fine | 164 | 41 | 130 |
| Coarse | 164 | 42 | 130 |

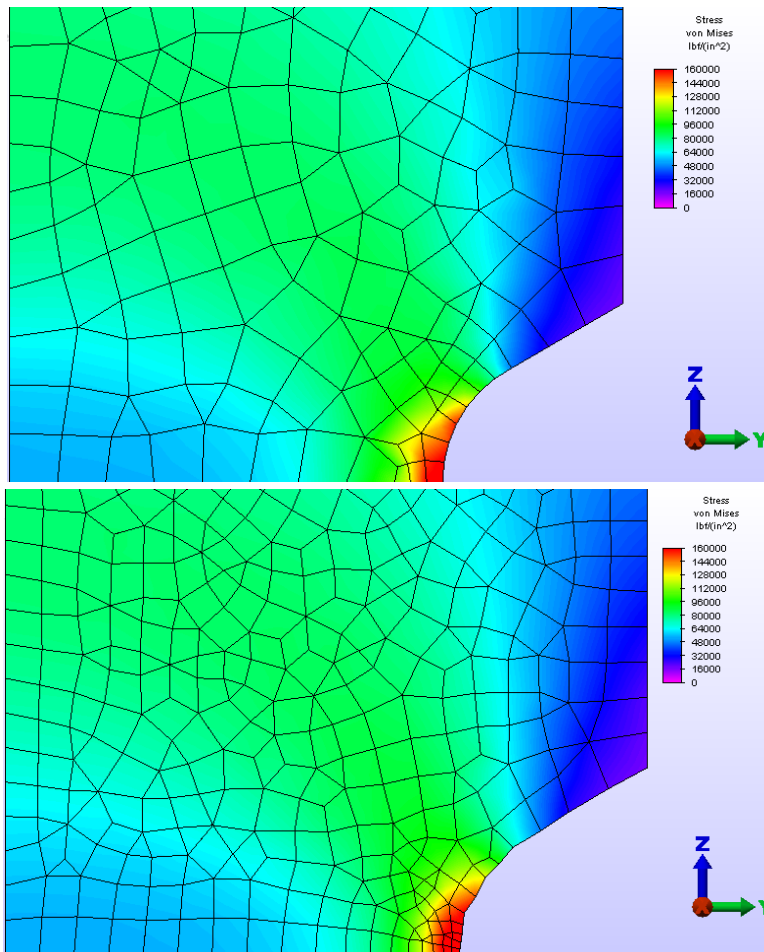


Figure 12.—Finer mesh size did not produce significant changes in stress levels at an applied net stress of 115 ksi. As seen in the table the maximum and minimum von Mises stress and the SWT stress did not change appreciably with mesh density.

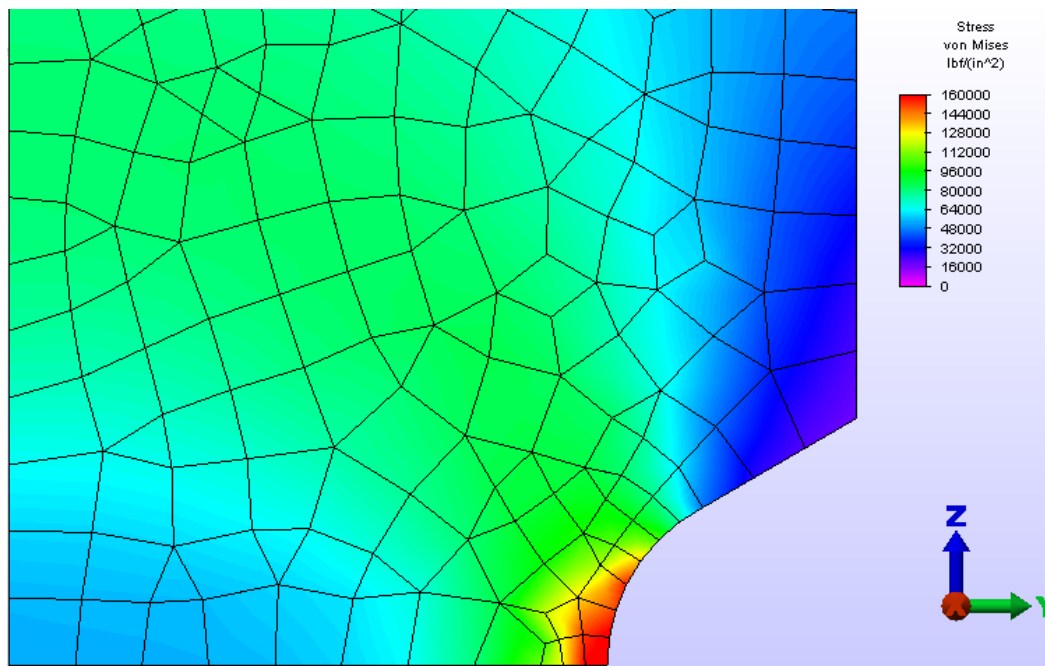
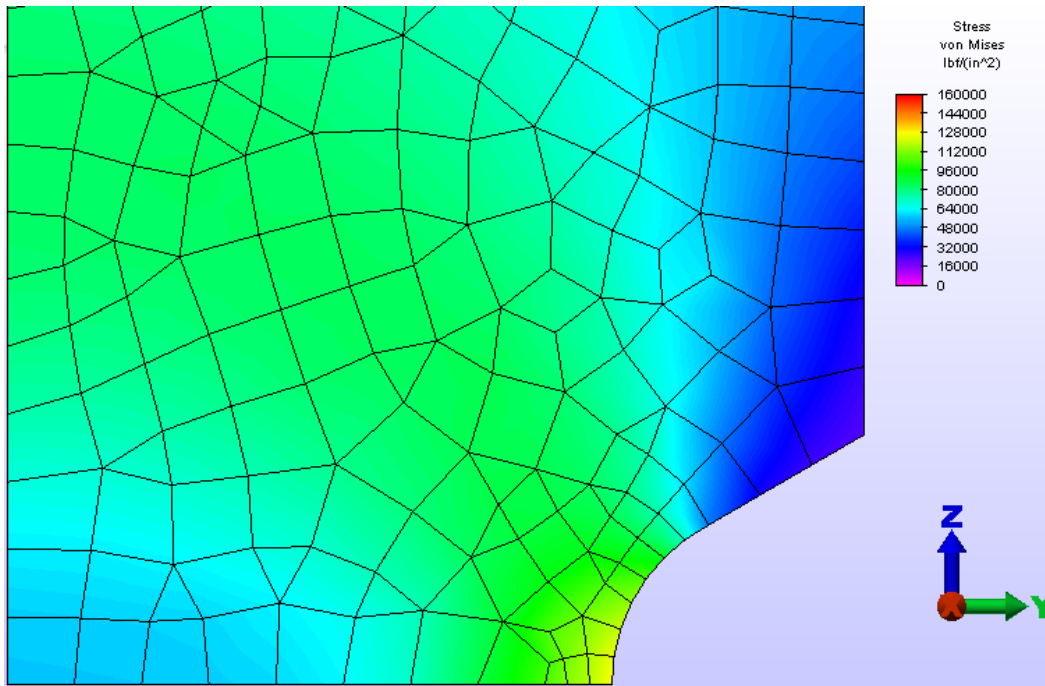


Figure 13.—Comparison of viscoplastic (top) and elastic-plastic analysis (bottom) for an applied load of 115 ksi.

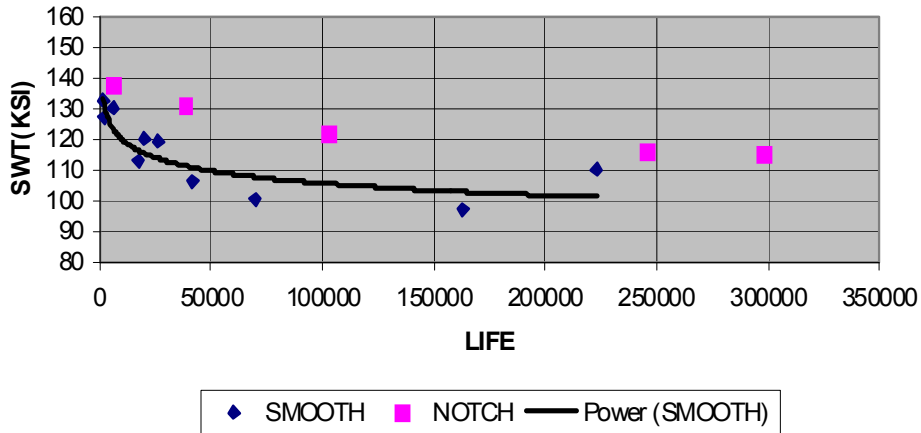


Figure 14.—1300 °F SWT fatigue life plot showing notch data based on viscoplastic finite element stress analysis.

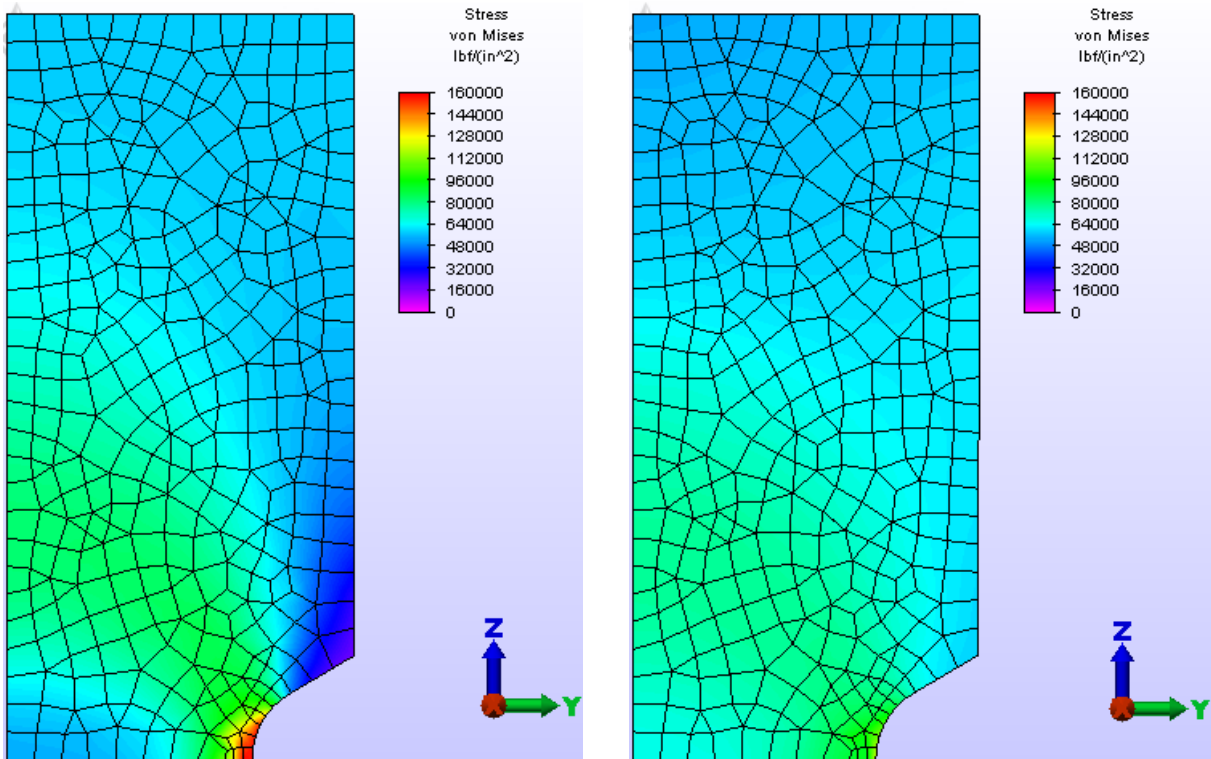


Figure 15.—Von Mises stress distribution at beginning (left) and end (right) of the 115 ksi notch dwell fatigue test. Stress distribution at peak load.

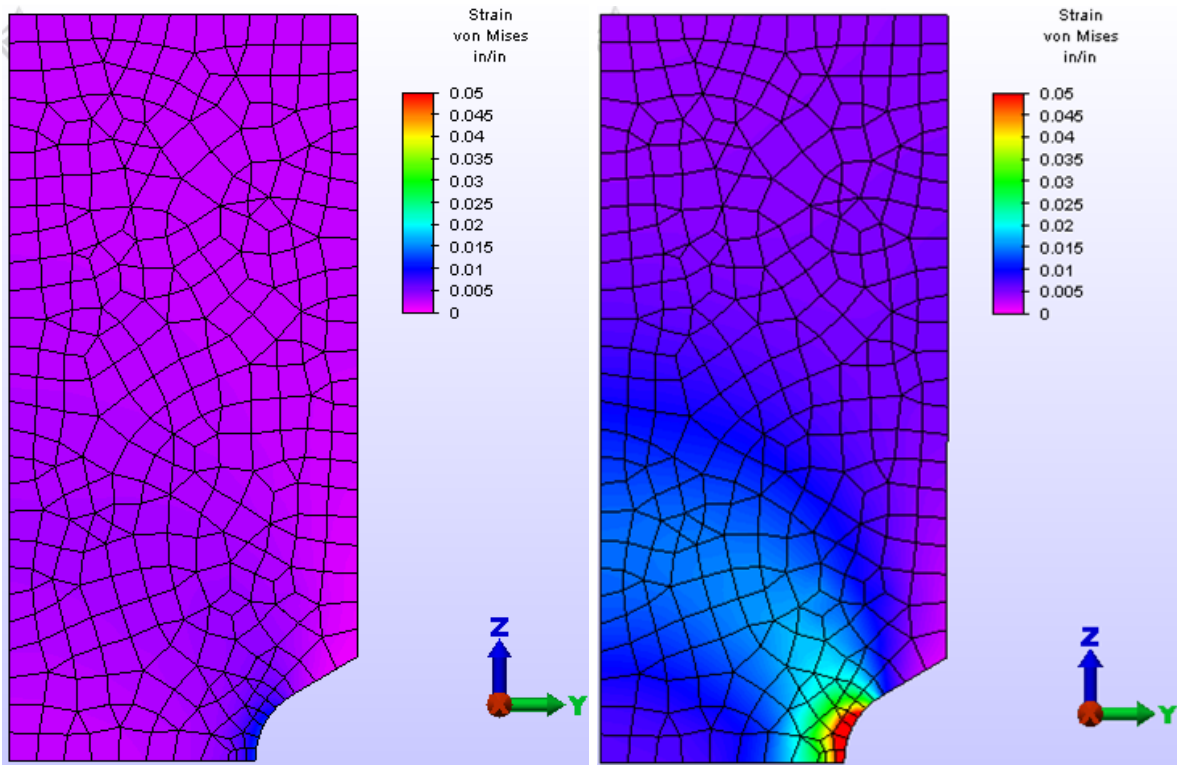


Figure 16.—Von Mises strain distribution at beginning (left) and end (right) of the 115 ksi notch dwell fatigue test. Strain distribution at peak load.

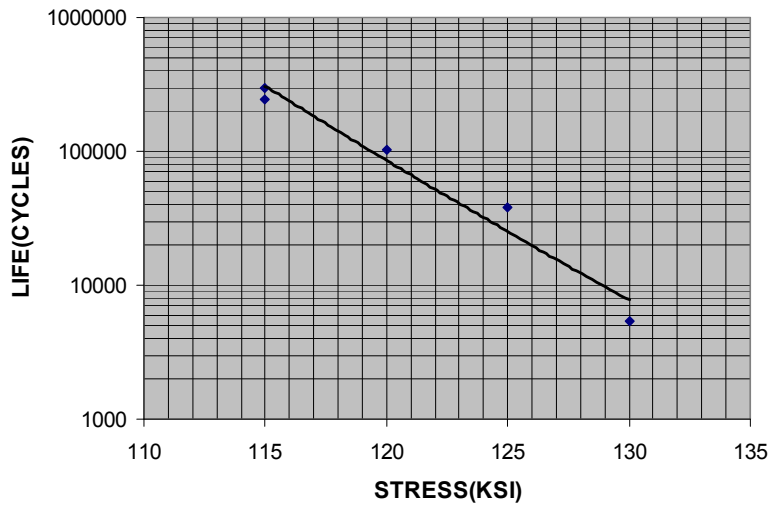


Figure 17.—1300 °F notch fatigue lives.

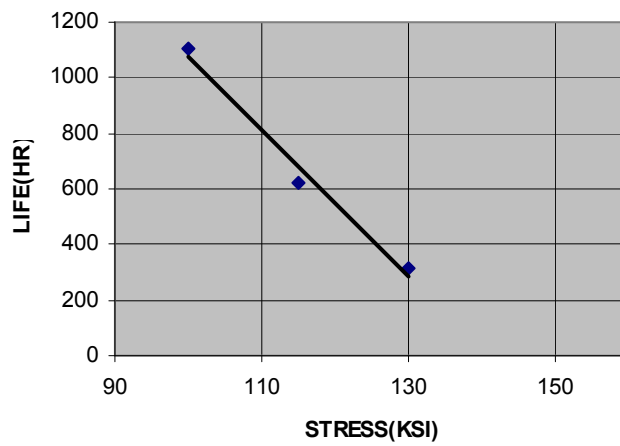


Figure 18.—1300 °F notch rupture lives.

REPORT DOCUMENTATION PAGE

Form Approved
OMB No. 0704-0188

The public reporting burden for this collection of information is estimated to average 1 hour per response, including the time for reviewing instructions, searching existing data sources, gathering and maintaining the data needed, and completing and reviewing the collection of information. Send comments regarding this burden estimate or any other aspect of this collection of information, including suggestions for reducing this burden, to Department of Defense, Washington Headquarters Services, Directorate for Information Operations and Reports (0704-0188), 1215 Jefferson Davis Highway, Suite 1204, Arlington, VA 22202-4302. Respondents should be aware that notwithstanding any other provision of law, no person shall be subject to any penalty for failing to comply with a collection of information if it does not display a currently valid OMB control number.

PLEASE DO NOT RETURN YOUR FORM TO THE ABOVE ADDRESS.

| | | | | | |
|--|--------------------|---|-----------------------------------|---|--|
| 1. REPORT DATE (DD-MM-YYYY) 01-10-2008 | | 2. REPORT TYPE Technical Memorandum | | 3. DATES COVERED (From - To) | |
| 4. TITLE AND SUBTITLE Fatigue Behavior of a Third Generation PM Disk Superalloy | | | | 5a. CONTRACT NUMBER | |
| | | | | 5b. GRANT NUMBER | |
| | | | | 5c. PROGRAM ELEMENT NUMBER | |
| 6. AUTHOR(S) Gayda, John; Gabb, Timothy, P. | | | | 5d. PROJECT NUMBER | |
| | | | | 5e. TASK NUMBER | |
| | | | | 5f. WORK UNIT NUMBER WBS 698259.02.07.03.04.02 | |
| 7. PERFORMING ORGANIZATION NAME(S) AND ADDRESS(ES) National Aeronautics and Space Administration John H. Glenn Research Center at Lewis Field Cleveland, Ohio 44135-3191 | | | | 8. PERFORMING ORGANIZATION REPORT NUMBER E-16655 | |
| 9. SPONSORING/MONITORING AGENCY NAME(S) AND ADDRESS(ES) National Aeronautics and Space Administration Washington, DC 20546-0001 | | | | 10. SPONSORING/MONITORS ACRONYM(S) NASA | |
| | | | | 11. SPONSORING/MONITORING REPORT NUMBER NASA/TM-2008-215462 | |
| 12. DISTRIBUTION/AVAILABILITY STATEMENT Unclassified-Unlimited Subject Category: 26 Available electronically at http://gltrs.grc.nasa.gov This publication is available from the NASA Center for AeroSpace Information, 301-621-0390 | | | | | |
| 13. SUPPLEMENTARY NOTES | | | | | |
| 14. ABSTRACT The fatigue behavior of a 3rd generation PM disk alloy, LSHR, was studied at 1300 °F. Tensile, creep, and fatigue tests were run on smooth and notched (Kt = 2) bars under a variety of conditions. Analysis of smooth bar fatigue data, run under strain and load control with R ratios of 0 and -1, showed that a stress based Smith-Watson-Topper approach could collapse the data set. While the tensile and creep data showed substantial notch strengthening at 1300 °F, the fatigue data showed a life deficit for the notch specimens. A viscoplastic finite element model, which accounted for stress relaxation at the notch tip, provided the best correlation between the notched and smooth bar behavior, although the fatigue data was not fully rationalized based on this simplified viscoplastic model of the stresses at the notch tip. Inclusion of a 90 sec dwell at peak load was found to dramatically decrease notch fatigue life. This result was shown to be consistent with a simple linear creep-fatigue damage rule, where creep damage dominated at low stresses and fatigue damage was more prevalent at higher stresses. | | | | | |
| 15. SUBJECT TERMS Superalloy; Disk; Fatigue | | | | | |
| 16. SECURITY CLASSIFICATION OF: | | | 17. LIMITATION OF ABSTRACT | 18. NUMBER OF PAGES | 19a. NAME OF RESPONSIBLE PERSON |
| a. REPORT | b. ABSTRACT | c. THIS PAGE | | | STI Help Desk (email: help@sti.nasa.gov) |
| U | U | U | UU | 22 | 19b. TELEPHONE NUMBER (include area code) 301-621-0390 |

